

Effect of Liquid Injection on Acoustic Field from Supersonic Flow Past Cavities

T. K. Ganesh Anavaradham*

Defence Research and Development Laboratory, Hyderabad 500 258, India

R. I. Sujith,[†] O. J. Shreenivasan,[‡] and S. R. Chakravarthy[§]

Indian Institute of Technology Madras, Chennai 600 036, India

and

S. Panneerselvam[¶]

Defence Research and Development Laboratory, Hyderabad 500 258, India

DOI: 10.2514/1.29832

This paper describes an experimental investigation of the effect of transverse liquid injection (distilled water) on the acoustic field generated by confined supersonic flow past a cavity. The effect of cavity depth in the absence/presence of liquid injection on the acoustic field is studied. In the presence of liquid injection, the effects of injection pressure and injection location on the acoustic field are investigated. The dependence of suppression/amplification of the acoustic amplitudes (compared with the absence of injection) on the injection condition and cavity depths is ascertained. In general, liquid injection in the presence of cavity resulted in higher amplitudes. Even square cavities that did not exhibit oscillations in the absence of injection generated significant acoustic amplitudes in the presence of liquid injection at high injection pressures. Phase-locked schlieren imaging was performed to sequence the fluid-dynamic events. Schlieren images indicate the interaction of the shock wave generated by the flow past the liquid jet and the oblique shock generated at the cavity-leading edge. The schlieren images show that the amplitude increase observed for higher injection pressures for a range of cavity depths is accompanied by an unsteady normal shock ahead of the cavity-leading edge (which does not span the entire width of the test model, but is located locally in front of the liquid jet).

I. Introduction

IN SUPERSONIC combustion ramjet engines (scramjets), due to the short residence times, it is essential to specifically adopt a device or strategy to enhance the mixing between the fuel and oxidizer to achieve combustors of reasonable size and weight. At the same time, the mixing device/strategy should not lead to large total pressure losses for the flow in the combustor, because this would lead to thrust losses. There are several techniques for improving the mixing. Some of them are based on the generation of streamwise vorticity, such as ramps, tabs, lobe mixers, chevrons, etc. Some others are based on the self-excitation of resonance such as with cavities. Seiner et al. [1] has presented a review of the history of adopting such mixing-enhancement techniques in scramjet engines.

Recent mixing-enhancement/flame-holding studies have concentrated on cavity-based devices as the total pressure losses incurred by these devices are less compared with other mixing-enhancement devices. Supersonic flow over cavities can excite acoustic oscillations, which can enhance the rate of mixing of fuel and oxidizer. Also, cavities provide a subsonic region containing a hot pool of combustion products, which can anchor the flame. The length of the

cavity determines the mass entrainment characteristics, whereas the depth of the cavity determines the residence time [2]. Therefore, cavities can be tuned to achieve either mixing enhancement or flame holding by changing the length and depth of cavity. It is then essential to understand the cavity behavior to incorporate cavities in scramjet engines.

Early research on cavities focused on studying the large fluctuating pressures occurring on the wall of the cavity because of its relevance to the flow in the weapon bays of aircraft [3]. A closed cavity usually has higher drag compared with an open cavity [4], and so the latter is preferred in scramjet engine applications. Krishnamurty [5], in his pioneering work on open cavities, reported the emission of acoustic radiation from cavities both in subsonic and supersonic flow. Rossiter [6] made a distinction between these cavities based on the predominance between random and periodic components of the observed oscillations in the subsonic-to-transonic regime. He has given an empirical formula for the prediction of the different modes as a function of the flow Mach number. Heller et al. [7] modified the Rossiter's formula recognizing the disparity in the speeds of sound in the freestream and within the cavity. However, neither formula contains an explicit dependence on the depth of the cavity.

The mechanism of self-sustained oscillations in a cavity has been a subject of debate until today. Various models have been proposed to model the physical processes in a cavity, namely, the interaction between pressure fluctuations and the acoustic source [6,8,9]. The results of Zhang and Edwards [10] showed open cavities to be dominated either by longitudinal or transverse oscillations depending on the L/D ratio and the Mach number. In the case of cavity with L/D less than 2, the oscillations are controlled by a transverse mechanism, whereas the oscillations are controlled by a longitudinal mechanism for cavity L/D greater than 2.

The work of Yu and Schadow [11] showed that the acoustic waves radiating from cavities are powerful enough to affect the mixing characteristics significantly. They demonstrated the enhancement of mixing in a freejet by a cavity mounted at the exit of the supersonic nozzle. They used two-dimensional and semicircular cavities. They found that the resonance causes periodic shedding of organized

Received 17 January 2007; revision received 28 December 2007; accepted for publication 14 January 2008. Copyright © 2008 by T. K. Ganesh Anavaradham, R. I. Sujith, O. J. Shreenivasan, S. R. Chakravarthy, and S. Panneerselvam. Published by the American Institute of Aeronautics and Astronautics, Inc., with permission. Copies of this paper may be made for personal or internal use, on condition that the copier pay the \$10.00 per-copy fee to the Copyright Clearance Center, Inc., 222 Rosewood Drive, Danvers, MA 01923; include the code 0748-4658/08 \$10.00 in correspondence with the CCC.

*Project Manager.

[†]Professor, Department of Aerospace Engineering; sujith@iitm.ac.in. Member AIAA.

[‡]Graduate Student and Project Officer, Department of Aerospace Engineering.

[§]Associate Professor, Department of Aerospace Engineering. Member AIAA.

[¶]Associate Director.

structures that can be used to control mixing. This could be achieved with the two-dimensional cavity only when the cavity dimensions were adjusted to specific acoustic modes. No adjustments were required for the semicircular type of cavity. Sato et al. [12] studied the effect of an acoustic wave impinging on the mixing layer. The primary air was supersonic with Mach number being 1.78, and the secondary air was injected from the injector installed on the center line of the nozzle. Their results showed that the combination of cavity shape and injector shape influences the mixing characteristics to a large extent. The impingement of acoustic wave improved the mixing of the main air and the injected air.

Burnes et al. [13] studied the effect of fuel injection on mixing using cavities with helium and tetrafluoroethane. They reported that the experiments provided direct evidence of persisting coherent structures in a ducted supersonic flowfield, which may enhance mixing. It was indicated that the fuel that was injected into the cavity suppressed the flow oscillations and inhibited the coherent structure formation, whereas fuel injected into the wake of the cavity was entrained into the coherent structures, showing evidence of mixing enhancement. Hsu et al. [14] conducted experiments using ethylene to measure quantitative fuel distributions around a cavity (fuel injected upstream of the cavity) in a nonreacting Mach 2 flow at different backpressures to simulate static pressure raise due to combustion. The boundary layer separated, causing a modification of the fuel transport to the cavity. They recommended that the fuel be delivered directly into the cavity for a controllable and stable cavity flame holder to eliminate the potential transition problem resulting from boundary-layer behavior. The last two papers showed contradictory requirements of fuel injection location for mixing enhancement and flame holding. Ben-Yakar and Hanson [15] discussed the need for an optimal configuration of cavity that will yield the most effective flame-holding capability and mixing enhancement with minimum losses in their study using hydrogen fuel.

In summary, cavities show great promise for mixing enhancement and also flame holding for scramjet applications. Although there is a large body of literature on the acoustic field produced by supersonic flow past a cavity, not much work has been done on investigating the influence of liquid injection on the cavity-induced acoustic field, and the influence of this acoustic field on the liquid penetration height and jet spread. In this context, it will be interesting to examine the acoustic amplitudes generated by the supersonic flow past a cavity, particularly when the liquid droplets from the fuel spray damp the acoustic field. This work examines the effect of liquid injection into supersonic flow past a cavity on the cavity dynamics and the resulting acoustic field. The effect of injector pressure and injection diameter on the acoustic field generated by the cavity is investigated. Phase-locked schlieren imaging are used to sequence the fluid-dynamic events occurring in the test section. The shock pattern in the presence and absence of liquid injection has been studied for different cavity depths.

II. Experimental Details

The experimental test facility has provision to supply compressed air at a maximum stagnation pressure of 10 bar from three reservoirs. The pipeline from the reservoir outlet was connected to a settling chamber, followed by a circular-to-rectangular transition duct (Fig. 1a). A Bourdon-type pressure gauge was used to monitor the stagnation pressure in the settling chamber, and the duct was connected to a 2-D convergent divergent nozzle. The nozzle was calibrated using a pitot-static probe, and the average Mach number (M_∞) is found to be 1.5 ± 0.05 (uncertainty of 3%). The static pressure at the exit of the nozzle is around 1 atm.

The nozzle was connected to the test section with a rectangular cross section of 40-mm height and 30-mm width. A schematic of the test model is shown in Fig. 1b. The length of the test model was maintained as 150 mm. A length of 150 mm was chosen, as previous investigations [16] showed that the acoustic signals were weak at locations far downstream of the cavity-trailing edge. On the top wall of the test section, three injection ports (P1, P2, and P3), and three transducer ports (T1, T2, and T3) for measuring acoustic pressure

were provided (Fig. 1b). The sides of the test model were made of glass for optical access and the top and bottom walls were made of acrylic sheets. The length of the cavity (L) was fixed as 50 mm, and the depth of the cavity was varied from 10 to 72 mm in steps of 2 mm. The cavity-leading-edge location is 50 mm from the start of test model. The cavity depth was varied by making the bottom wall of the cavity movable. A cavity length of 50 mm was chosen from the numerical simulation results [17] because the amplitudes are the highest for a cavity length of 50 mm as compared with other cavity lengths. A cavity depth less than 10 mm does not produce any significant acoustic oscillation, and a cavity depth more than 70 mm cannot be accommodated in a practical supersonic combustor. Therefore, a depth range of 10 to 72 mm was selected for the study. The Mach wave (angle of 42 deg with respect to freestream flow) corresponding to freestream Mach number of 1.5 is shown in Fig. 1b.

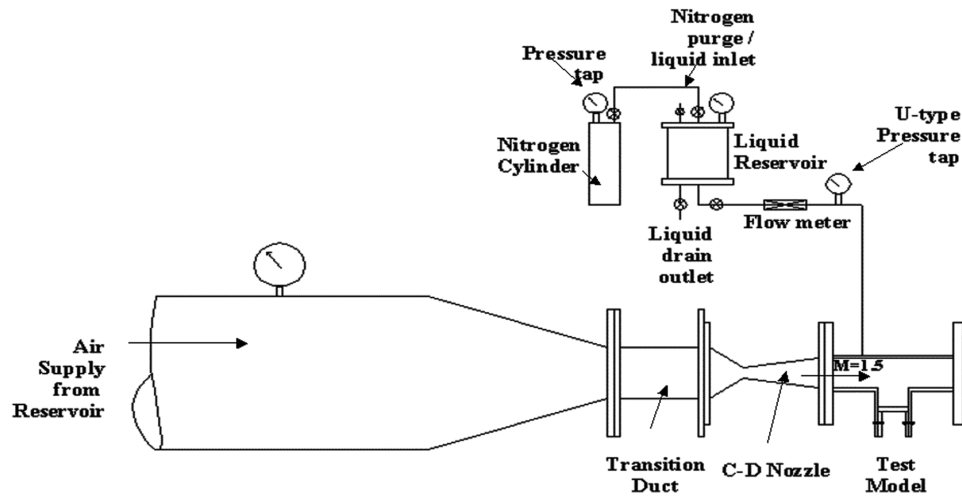
The three injection locations were located such that the P1 injection location was ahead of the cavity-leading edge on the wall opposite to cavity, the P2 location was directly opposite to the cavity-leading edge, and the P3 location was slightly downstream of the cavity-leading-edge location. The injector diameters chosen were 1 mm and 0.8 mm. The injector was made of stainless steel, and it is a plain orifice injector mounted flush with the inner wall of the test model. Distilled water was used as the surrogate fuel. Nitrogen cylinders were used to pressurize the liquid stored in a cylindrical tank. A flow-regulating valve was connected to the nitrogen cylinder to get different injection pressures (i.e., to reduce the 150-bar pressure in the nitrogen cylinder to the required injection pressure). A Bourdon type pressure gauge was installed in the line from the outlet valve in the tank to the injector to measure the injection pressure.

The acoustic pressure measurements were performed on the wall opposite to the cavity using Kistler type 206 piezoelectric transducers. The transducer has a sensitivity of 100 mV/psi, with a dynamic pressure range of 0.01–80 psi at any static pressure level. The transducer location T1 was located just ahead (20 mm) of the Mach wave impingement location on the top wall. It was seen in numerical simulations for the case of absence of injection [16] that unsteadiness was not experienced at locations (around 30 mm) ahead of the Mach wave impingement location. Therefore, transducers were not located ahead of the T1 location. The signal from the transducer is conditioned using a signal conditioner and acquired using a computer through a 12-bit analog-to-digital (A/D) data acquisition board, which can sense signals up to a maximum peak-to-peak voltage level of 5 V. The maximum uncertainty in the measurement of the acoustic pressure amplitude due to digitization is 7 Pa. The amplitude nonlinearity of the transducer is $\pm 1\%$ in the calibrated range. Because the dominant frequency to be measured is estimated as in the 4–25 kHz range, the sampling frequency is set at 100 kHz. The number of samples acquired is 32,768 ($=2^7$). Fast Fourier transform (FFT) is performed on the stored signal with a frequency resolution of 3 Hz. The output of the FFT is used to determine the frequency components and its amplitude.

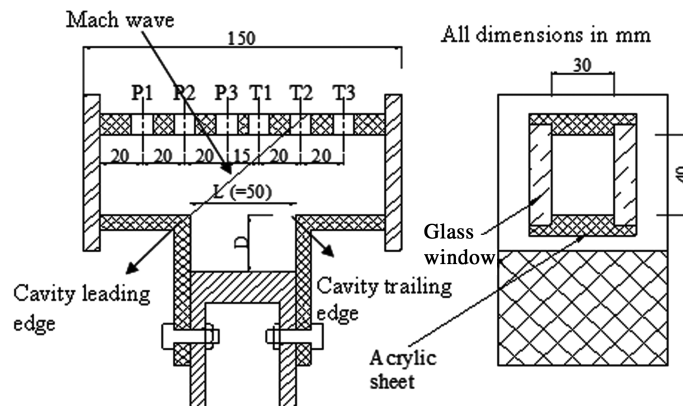
III. Results and Discussion

A. Acoustic Field in Absence of Injection

Acoustic signals were acquired at three locations (T1, T2, T3) in the absence of injection (baseline case) for different cavity depths. The amplitude spectrum for four different cavity depths ($D = 0$ mm; i.e., absence of cavity, 24, 40, 68 mm) acquired at T1 location is shown in Fig. 2. In the absence of cavity, the spectrum is broadband with low amplitudes indicating that the flow is steady. In the presence of cavity, the signals consisted of broadband frequencies accompanied by a narrow band of preferred frequencies (tones) with considerable amplitude. Discrete tones with high acoustic amplitudes are observed for shallow and deep cavities. However, tones are not observed for the case of square cavities at T1 transducer location (D in the range of 40–56 mm). The shallow cavities exhibited two or three discrete tones at frequencies less than 10 kHz. In the case of deep cavities, three or four discrete tones exist with the higher discrete frequencies being in the range of 10–20 kHz. Also,



a) Experimental test facility



b) Schematic of test model showing injection and transducer locations

Fig. 1 a) Experimental test facility. b) Schematic of test model showing injection and transducer locations.

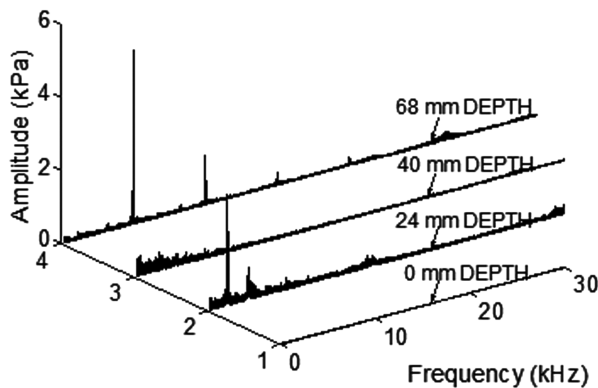


Fig. 2 Amplitude spectrum in the absence of liquid injection at T1 measurement location for various cavity depths.

the dominant frequency jumps to a higher value when the cavity geometry changes from shallow to deep cavity.

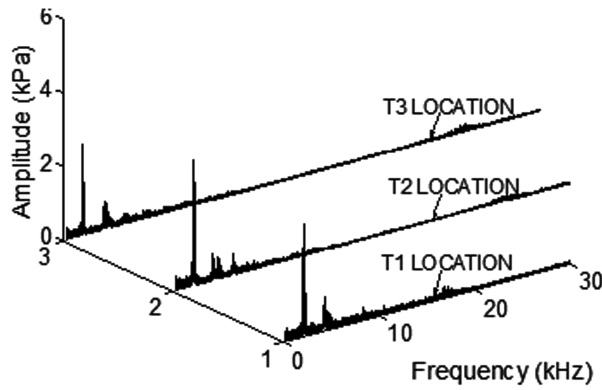
The amplitude spectrum at the three locations (T1, T2, and T3) for a cavity depth of 24, 40, and 68 mm are given in Figs. 3a–3c. The maximum amplitude was experienced at T1 location for the cavity depth of 24 mm (Fig. 3a) and is nearly of the same magnitude as that at T2 location, whereas it decreases at T3 location. The T1 location was located downstream of the oblique shock (generated by the cavity-leading edge) impingement location on the top wall. The T3 transducer will register the fluid-dynamic effects generated at cavity-trailing edge in addition to cavity-leading-edge effect. The cavity-trailing edge will have oblique shocks/expansion waves because of

the oscillation of the shear layer near the trailing edge location. These effects were weak for a cavity depth of 24 mm, resulting in reduced amplitudes at T3 location. The amplitude spectrum for cavity depth of 68 mm (Fig. 3c) shows maximum amplitude at T3 location. The magnitude of amplitude at T1 location is comparable to amplitudes registered at T3 location. The amplitude experienced for cavity depth of 40 mm (Fig. 3b) was much lower than in the case of cavities with 24 or 68 mm depth. This is consistent with the observation that square cavities do not produce strong acoustic fields as compared with shallow and deep cavities.

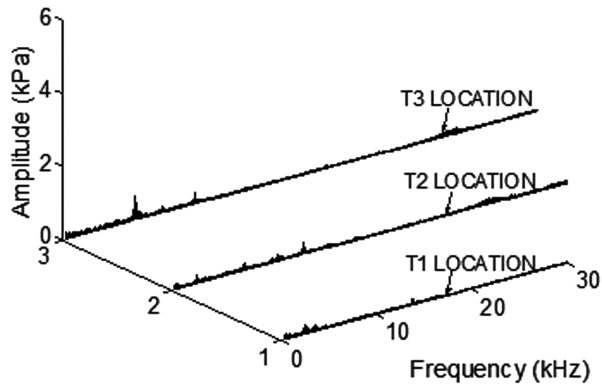
Schlieren images showed that in general, shallow cavities experienced large scale vortices moving upstream inside the cavity and large shear-layer deflections near the cavity-leading edge and deep cavities showed small-scale vortices convected downstream, with large shear-layer deflections near the cavity-trailing edge [17].

B. Acoustic Field in Presence of Injection

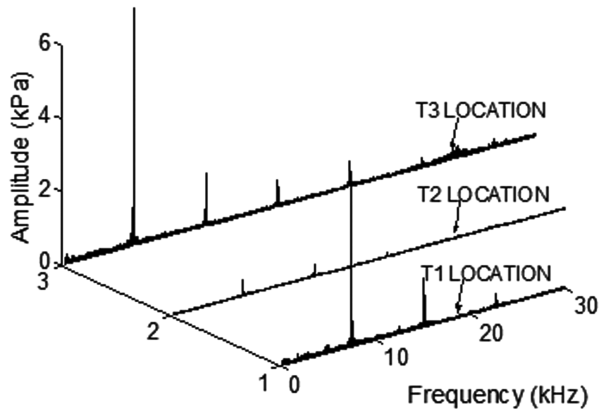
Experiments were performed with distilled water injection from an injector of 1 mm in diameter located at the P3 location that is located 25 mm downstream of the cavity-leading edge. Acoustic data was first acquired in the absence of cavity, with liquid injection at different pressures. The amplitude of oscillations is approximately 20 Pa, indicating that in the absence of cavity, liquid injection does not lead to any significant acoustic field. The amplitude spectrum (at T1 location) for different cavity depths at 5-bar injection pressure is shown in Fig. 4. It can be seen in Fig. 4 that the periodic pressure fluctuations of considerable acoustic amplitudes are experienced for shallow cavities (D is 16–32 mm) and deep cavities (D is 66–72 mm) in spite of the acoustic damping by the droplets, whereas broadband spectrum is observed for square cavities (D is 40–66 mm). The amplitudes are highest for a cavity depth of 24 mm and two to three



a)



b)



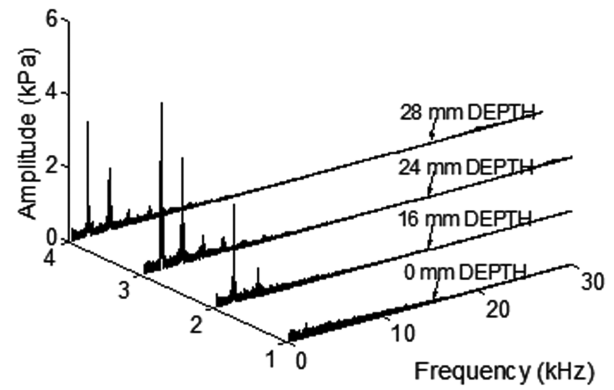
c)

Fig. 3 Amplitude spectra at different locations in the absence of liquid injection for cavity depths of a) 24 mm, b) 40 mm, and c) 68 mm.

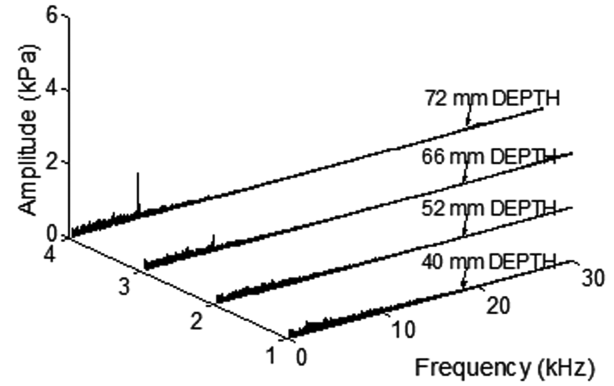
discrete tones could be seen in the amplitude spectrum. Similar trends in spectra are observed from the acoustic pressure measurements at T2 and T3 locations.

The amplitude spectrum of different cavity depths for the 20-bar injection pressure is shown in Fig. 5 for the T1 location. The amplitudes for 20-bar injection pressure increased substantially compared with the case of absence of injection and 5-bar injection pressure. Maximum amplitude (of the order of 12 kPa) is observed for a cavity depth of around 28 mm. Square cavities (depth around 40 mm) that did not produce significant amplitudes in the absence of injection now produced amplitudes of the order of 7 kPa in the presence of injection. The measurement of pitot pressure at the exit of the test section could not be performed due to water droplets getting into the probe. The reasons for the changes in frequencies of oscillations and the corresponding amplitudes are discussed with the help of phase-locked schlieren images.

Phase-locked schlieren images were used to sequence the fluid-dynamic events. The phase-locked images for a cavity depth of

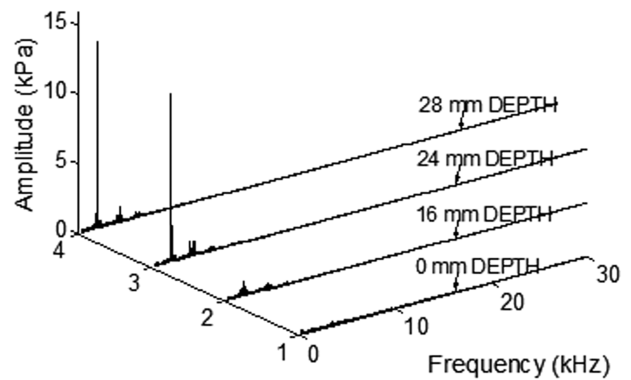


a)

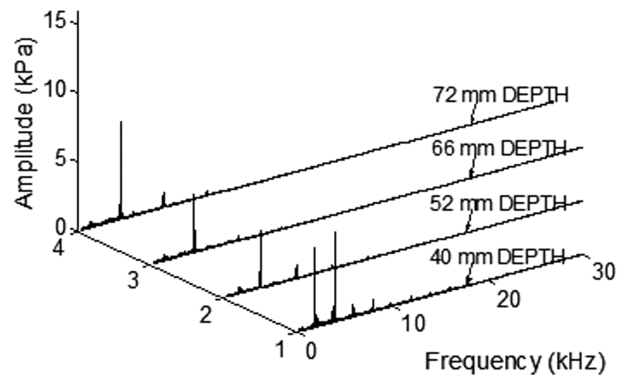


b)

Fig. 4 Amplitude spectra at T1 location for P3 injection with an injection pressure of 5 bar for various cavity depths.



a)



b)

Fig. 5 Amplitude spectra at T1 location for P3 injection with an injection pressure of 20 bar for various cavity depths.

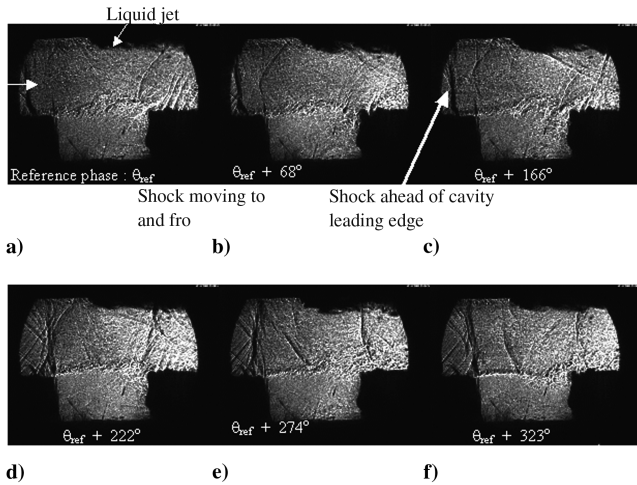


Fig. 6 Phase-locked, instantaneous schlieren images for a cavity depth of 24 mm at an injection pressure of 5 bar and P3 injection.

24 mm at 5-bar injection pressure are shown in Fig. 6. The images were phase locked at a frequency of 2.1 kHz. The images show a highly unsteady normal shock standing ahead of the cavity-leading edge during a part of the cycle (Figs. 6a–6c). The normal shock does not span the entire width (the width of the test model is 30 mm and the width of the liquid jet will be less than 5 mm), but is present only in front of the liquid jet and that the area averaged Mach number will be supersonic. The blockage offered by the liquid jet is estimated to be less than 4% of the test section area without cavity. During the other part of the cycle, the oblique shock generated at the cavity-leading edge wave interacts with the shock generated by the supersonic flow past the liquid jet (Figs. 6d–6f). The shear layer undergoes oscillations, and during the cycle, the shear-layer deflection at the cavity-leading edge increases and then decreases. Shock waves could be seen near to the cavity-trailing edge (Fig. 6d).

The phase-locked instantaneous schlieren images for the cavity depth of 24 mm with injection pressure of 20 bar are shown in Fig. 7. These images were phase locked at a frequency of 2.01 kHz. Only a few schlieren images show normal shock (it is inferred that in the remaining images, the shock is located far upstream of the cavity-leading edge, which could not be captured due to limitations in schlieren window size), and the normal shock is highly unsteady. The normal shock could be seen in Figs. 7e, 7g, and 7i, and the normal shock resulted in changing the flow conditions at the cavity-leading edge resulting in increased amplitudes. A weak wave could be seen on the shear layer (Figs. 7a, 7b, and 7k), and strong shocks could be witnessed after the cavity-trailing edge (Figs. 7j–7l). The obstruction offered by the injected liquid (estimated to be less than 7% of the test section area without the cavity) at 20-bar injection pressure will create a strong shock compared with 5-bar injection pressure because of the increased mass flow rate of the injected liquid. The increased static pressure and reduction in Mach number at the cavity-leading edge resulted in increased amplitudes. Similarly, the unsteady normal shock that was located in front of the liquid jet was found to occur for injection pressures of 10 and 15 bar, resulting in increased amplitudes compared with the absence of injection.

The amplitude spectrum for the cavity depth of 40 mm showed frequencies of oscillations with significant amplitudes (of the order of 7 kPa) at 20-bar injection pressure (Fig. 5b). In this case, the supersonic flow past the cavity did not generate significant amplitudes in the absence of injection, whereas it generated significant amplitudes at high injection pressures because of the interaction occurring between the shock generated by the flow past the liquid jet and the shock wave at the cavity-leading edge. The instantaneous schlieren image is shown for cavity depth of 40 mm in Fig. 8a for 5-bar injection pressure and in Fig. 8b for 20-bar injection pressure. The presence of an oblique shock at the cavity-leading edge and the shock generated by flow past the liquid jet could be seen at 5-bar injection pressure. Instantaneous schlieren image for 20-bar injection pressure (Fig. 8b) shows the absence of oblique shock at

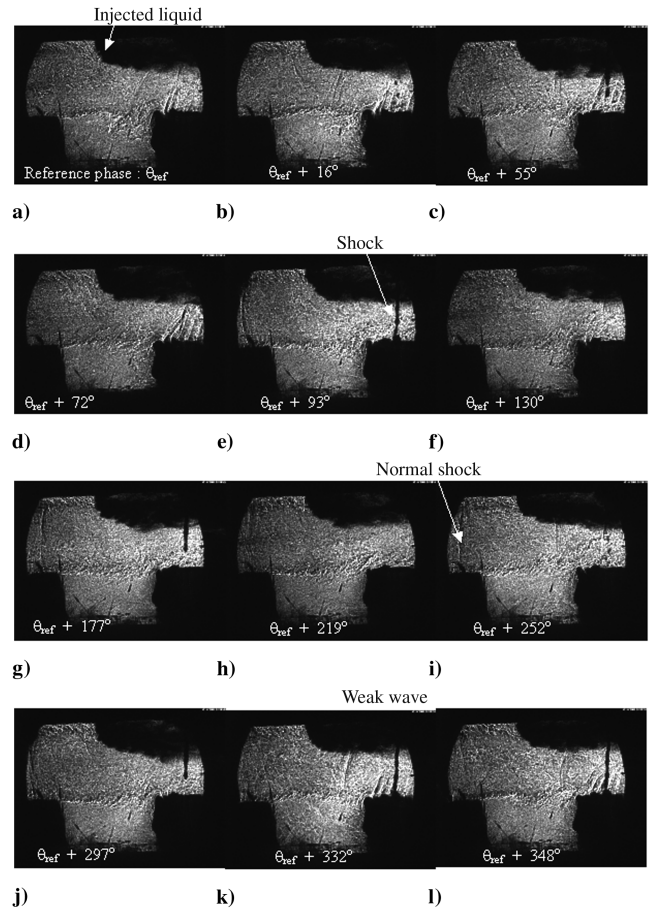


Fig. 7 Phase-locked, instantaneous schlieren images for a cavity depth of 24 mm at an injection pressure of 20 bar and P3 injection.

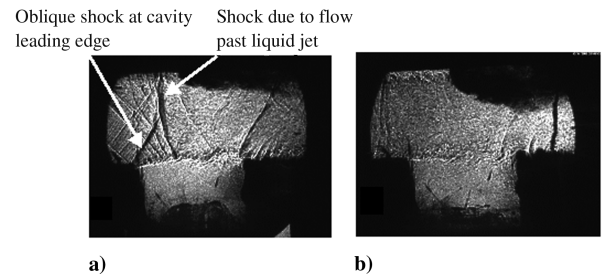


Fig. 8 Instantaneous schlieren images for cavity depth of 40 mm (P3 injection) at injection pressure of a) 5 bar and b) 20 bar.

cavity-leading edge and a normal shock standing ahead of the cavity-leading edge.

The phase-locked instantaneous schlieren images for cavity depth of 66 mm at 10-bar injection pressure is shown in Fig. 9. The images were phase locked at a frequency of 4.8 kHz. These schlieren images indicate the oscillation of shear layer with vortices being convected downstream along the shear layer. During a part of the cycle, the shear layer bends towards the cavity-trailing edge, and a shock is generated (Fig. 9d) ahead of the cavity-trailing edge. During the other part of the cycle, the shear layer flows over the cavity-trailing edge, and a shock gets formed (Fig. 9g) at a location downstream of the trailing edge. Unlike the case of shallow cavities, the normal shock is not seen in the images.

These results indicate that, for shallow cavities, even an injection pressure of 10 bar resulted in increased amplitudes, and the schlieren images show a normal shock ahead of the cavity-leading edge. In the case of square and deep cavities, high injection pressures (around 20 bar) resulted in increased amplitudes compared with the case of absence of injection.

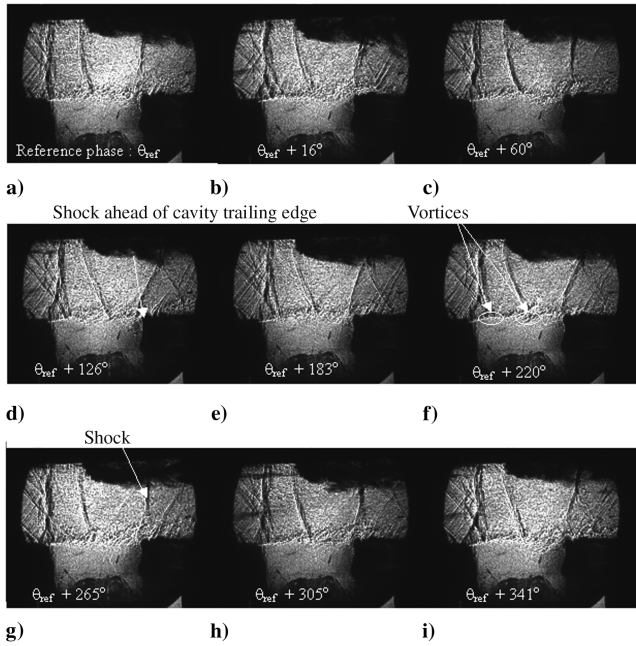


Fig. 9 Phase-locked, instantaneous schlieren images for a cavity depth of 66 mm at an injection pressure of 10 bar (P3 injection).

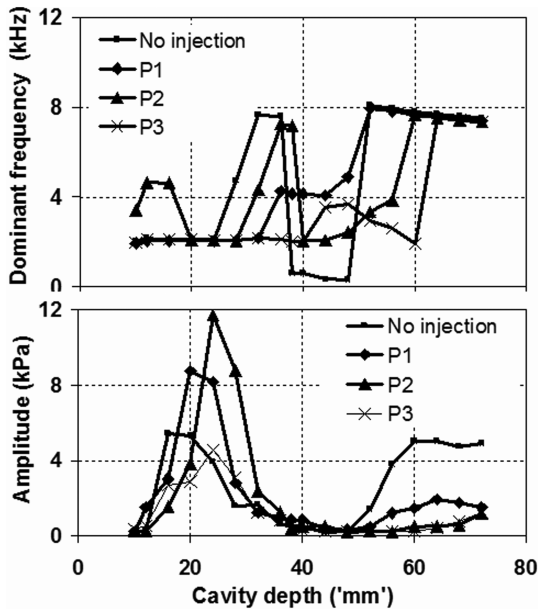


Fig. 10 Dominant frequency and amplitude for the case of absence/presence of injection at different injection locations for varying cavity depths (5-bar injection pressure).

The changes in injection location and injection diameter changed the magnitude of the acoustic oscillations; however, the behavioral pattern in terms of increased amplitudes at higher injection pressures compared with case of absence of injection is the same irrespective of the changes in injection location or diameter. A detailed presentation of these results is available in [17].

The dominant frequency and the corresponding amplitude for different cavity depths are consolidated and shown in Fig. 10 for injection pressures of 5 bar. In the absence of injection, the flow past cavity depths less than 10 mm did not generate an acoustic field of significant amplitudes. In the absence of injection, two mode jumps are experienced as the cavity nature changes from shallow to square and from square to deep cavity. Around a depth of 28 mm, the dominant frequency shifts from the first mode (i.e., first discrete frequency) to the third mode accompanied by reduction in

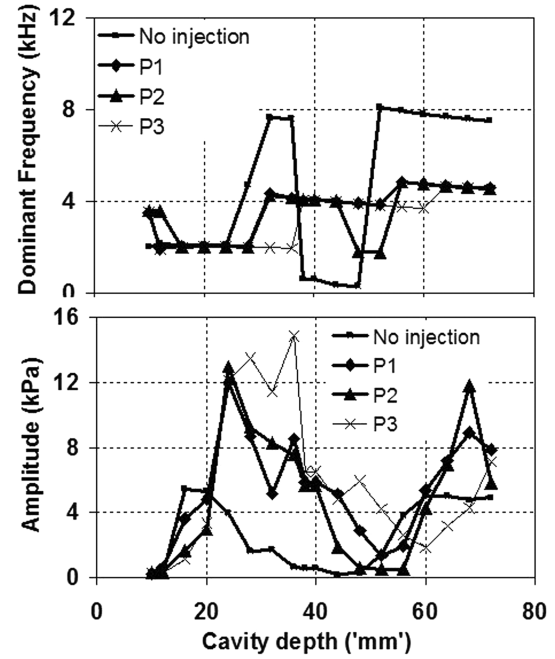


Fig. 11 Dominant frequency and amplitude for the case of absence/presence of injection at different injection locations for varying cavity depths (20-bar injection pressure).

amplitudes. Around 40–50-mm cavity depth, the flow does not show discrete frequencies with significant amplitudes. When the cavity becomes a deep cavity, the second mode dominates the oscillations, and the amplitudes are comparable with the case of shallow cavity. In the case of injection, the mode jumps (i.e., from first mode to third mode and then from third mode to second mode) occurs at higher cavity depths. The first mode jump that occurred around 28 mm in the case of absence of injection occurred around 40 mm for 5-bar injection pressure (P3 injection location). The second mode jump occurred at 60 mm cavity depth instead of 50 mm cavity depth as in the case of absence of injection. The only injection location that suppressed the amplitudes (as compared with the case of absence of injection) for shallow cavities was the P3 injection location. The other two injections resulted in increased amplitudes for shallow cavities and the amplitudes are suppressed irrespective of the injection location for deep cavities.

The dominant frequency and amplitudes for 20-bar injection pressure at different injection locations are given in Fig. 11. The amplitudes increased over the case of absence of injection for the cavity depth ranging from 20–48 mm and from 62–72 mm. It can be seen that cavities that did not generate acoustic amplitudes in the case of absence of injection, now produced significant amplitudes for all the three injection locations. The shock generated by the flow past the liquid jet changes the Mach number at the cavity-leading edge, resulting in changes in the dominant frequency. There are a few cavity depths around 55 mm (L/D slightly greater than 1), which did not show any increase in amplitude compared with the case of absence of injection.

On the whole, the liquid injection resulted in increase in amplitudes and shift in dominant frequencies. Instantaneous schlieren images indicate interaction of the shock waves generated by flow past the liquid jet and the cavity. In those cavities in which injection leads to large amplitudes, a normal shock could be seen ahead of the cavity-leading edge, and it is not stable. During the cycle, a normal shock is seen traveling back and forth in the constant area portion ahead of the cavity-leading edge.

IV. Conclusions

Experimental investigation was performed to study the effect of liquid injection (distilled water as surrogate fuel) on acoustic radiation of a rectangular wall-mounted cavity in confined supersonic

cross flow. The effect of cavity depth, liquid-injection pressure, and injection location on the acoustic field was studied with the supersonic flow Mach number being 1.5. The acoustic amplitudes generated by flow past the cavity in the presence of liquid injection increased substantially compared with the case of absence of injection, in spite of the acoustic damping by the droplets. The increased amplitudes occurred for the entire cavity depths tested for an injection pressure of 20 bar (except for a few cavity depths around 55 mm). The shock induced due to flow past the liquid jet changes the cavity-leading-edge flow conditions, resulting in changes in the acoustic field. Instantaneous phase-locked schlieren images were obtained to visualize the shock structures generated due to liquid injection and its interaction with the shock structures generated by the cavity. The increased amplitudes could be attributed to the unsteady normal shock standing ahead of the cavity-leading edge. The normal shock does not span the width of the model but is present only in front of the liquid column.

References

- [1] Seiner, J. M., Dash, S. M., and Kenzakowski, D. C., "Historical Survey on Enhanced Mixing in Scramjet Engines," *Journal of Propulsion and Power*, Vol. 17, No. 6, 2001, pp. 1273–1286.
- [2] Baurle, R. A., and Gruber, M. R., "A Study of Recessed Cavity Flowfields for Supersonic Combustion Applications," AIAA Paper 98-0938, 1998.
- [3] Rockwell, D., and Naudascher, E., "Review: Self Sustaining Oscillations of Flow Past Cavities," *Journal of Fluids Engineering*, Vol. 100, No. 6, 1978, pp. 152–165.
- [4] Baysal, O., and Stallings, R. L., Jr., "Computational and Experimental Investigation of Cavity Flowfields," *AIAA Journal*, Vol. 26, No. 1, 1988, pp. 6–7.
- [5] Krishnamurty, K., "Acoustic Radiation from Two-Dimensional Rectangular Cutouts in Aerodynamic Surfaces," NACA TN 3487, 1955.
- [6] Rossiter, J. E., "Wind Tunnel Experiments on the Flow over Rectangular Cavities at Subsonic and Transonic Speeds," R&M No. 3438, 1966.
- [7] Heller, H. H., Holmes, D. G., and Covert, E. E., "Flow Induced Pressure Oscillations in Shallow Cavities," *Journal of Sound and Vibration*, Vol. 18, No. 4, 1971, pp. 545–553.
doi:10.1016/0022-460X(71)90105-2
- [8] Tam, C. K. W., and Block, P. J. W., "On the Tones and Pressure Oscillations Induced by Flow over Rectangular Cavities," *Journal of Fluid Mechanics*, Vol. 89, No. 2, 1978, pp. 373–399.
doi:10.1017/S0022112078002657
- [9] Takakura, Y., Suzuki, T., Higashino, F., and Yoshida, M., "Numerical Study on Supersonic Internal Cavity Flows: What Causes the Pressure Fluctuations?," AIAA Paper 99-0545, 1999.
- [10] Zhang, X., and Edwards, J. A., "An Investigation of Supersonic Oscillatory Cavity Flows Driven by Thick Shear Layers," *The Aeronautical Journal*, Vol. 94, No. 940, 1990, pp. 355–364.
- [11] Yu, K. H., and Schadow, K. C., "Cavity-Actuated Supersonic Mixing and Combustion Control," *Combustion and Flame*, Vol. 99, No. 2, 1994, pp. 295–301.
doi:10.1016/0010-2180(94)90134-1
- [12] Sato, N., Imamura, R., Shiba, S., Takahashi, S., Tsue, M., and Kono, M., "Advanced Mixing Control in Supersonic Airstream with a Wall Mounted Cavity," *Journal of Propulsion and Power*, Vol. 15, No. 2, 1999, pp. 358–360; also AIAA Paper 96-4510, 1996.
- [13] Burnes, R., Parr, T. P., Wilson, K. J., Yu, K., "Investigation of Supersonic Mixing Control using Cavities: Effect of Fuel Injection Location," AIAA Paper 2000-3618, 2000.
- [14] Hsu, K. Y., Carter, C., Crafton, J., Gruber, M., Donbar, J., Mathur, T., Schommer, D., and Terry, W., "Fuel Distribution About a Cavity Flameholder in Supersonic Flow," AIAA Paper 2000-3585, 2000.
- [15] Ben-Yakar, A., and Hanson, R. K., "Cavity Flameholders for Ignition and Flame Stabilization in Scramjets: An Overview," *Journal of Propulsion and Power*, Vol. 17, No. 4, 2001, pp. 869–877.
- [16] Ganesh Anavaradham, T. K., Umesh Chandra, B., Babu, V., Chakravarthy, S. R., and Panneerselvam, S., "Experimental and Numerical Investigation of Confined Unsteady Supersonic Flow over Cavities," *The Aeronautical Journal*, Vol. 108, No. 1081, 2004, pp. 135–144.
- [17] Ganesh Anavaradham, T. K., "Investigation of Cavity Dynamics and its Interaction with Liquid Jet in Confined Supersonic Flow," Ph.D. Thesis, Indian Institute of Technology Madras, Chennai, India, 2006.

R. Bowersox
Associate Editor